Mass transfer and kinetic studies on mercury adsorption by titania nanofibers

Abhilasha Dixit[1], P. K. Mishra[2] and M. S. Alam[1]

[1]*Department of Chemical Engineering, Motilal Nehru National Institute of Technology, Allahabad, UP, India-211004*
[2]*Department of Chemical Engineering, Indian Institute of Technology (BHU), Varanasi, UP, India-221005*

Abstract. The stringent laws and tight regulation on heavy metal bearing wastewaters being discharged into the water stream lead to emergence of technically advanced and super effective treatment methods. Heavy metal contaminated aqueous streams have become a global concern due to their carcinogenicity and delirious effects on human health. In particular, the health hazards of mercury include adverse effect on central nervous system, pulmonary and kidney functions, etc. Having a maximum discharge limit of 0.001 mg/L, which is the lowest amongst other heavy metals, mercury contamination has become a matter of global concern. In the present study, TiO_2 having a proven track record for its affinity for heavy metals was lab synthesized in the form of fiber mats and tested for its adsorptive behaviour towards Hg(II) in aqueous system. The electrospinned nanofibers possessed smooth morphology and very high surface area ≈ 740 m^2/g. The batch adsorption experiments showed titania nanofibers possessed great affinity towards Hg(II). At the most optimized conditions the removal percentage went remarkably high to 95.5% with initial Hg(II) concentration of 0.01 mg/L. Since the rate limiting steps in adsorption are of vital importance in order to define the rate parameters for design purposes, the present study takes into account External mass transfer, Weber and Morris and Boyd mass transfer diffusion models for Hg(II) adsorption on lab synthesized titania nanofibers. The equilibrium data were then analyzed using Langmuir, Freundlich and Temkin sorption models and the characteristic sorption parameters for each isotherm were determined. The Mass transfer mechanism appeared to be film diffusion controlled and data fitted best to Freundlich isotherm with regression value of 0.991. The discussion also focuses on few of the recently used adsorbents for Hg(II) uptake and their comparison with the present study on the basis of removal percentage and kinetics involved. Promising adsorbent characteristics and rapid Hg(II) uptake makes this process a convenient one.

1 Introduction

Water pollution affects the entire biosphere and so is a problem of great concern. The increasing industrialization has played a very important in the degradation of natural water resources. The direct or indirect discharge from the industries into the water bodies demote the water quality and make it unsuitable for aquatic as well human life. Metals reach the environment naturally through the weathering of soils and rocks, and through anthropogenic activities like mining, processing, etc.

Mercury with a maximum discharge limit of 0.001 mg/L is considered to be a global pollutant. Its presence in environment is of significant concern because of its extreme toxicity, persistence and bioaccumulation properties [1]. Once in the environment, mercury gets converted into methyl-mercury chloride, which is its most toxic form. The major industries releasing mercury-laden wastewaters into environment are fertilizers, mining, mineral processing and tanning, etc. human exposure to mercury has severe health affects like neurological imbalance, anxiety, restlessness and lung disease, etc. Techniques like chemical precipitation and ion exchange for heavy metal remediation have their own respective disadvantage of sludge production and being economically infeasible.

Adsorption with its advantage of operation and design flexibility has come up as a very promising technique for heavy metal uptake. Numerous studies have highlighted the efficient use of modified activated carbons [2], chitosan [3], carbon nanotubes [4], etc for heavy metal adsorption. The advantage of using nano adsorbents for heavy metal remediation from wastewaters lies in their properties such as high porosity and enhanced structural properties suitable for adsorption process. Nanostructured metal oxide materials have attracted considerable attention because of their potential applications in many areas such as electronics, photonics, sensors and catalysis [5-7]. Nanosized ceramics with large surface area per unit mass can have enhanced electrical, physical, and chemical properties with respect to their bulk counterparts [8]. Nanofibers are an excellent new class of materials being used for numerous applications such as insulation, medical, cosmetics and filtration, etc. Various

approaches for preparation of nano and microstructures of titania have been reported, such as sol-gel processes, pyrolysis, electrospinning, chemical vapor deposition and hydrothermal methods [9-11]. Electrospinning has recently attracted much attention for nano-fiber synthesis since it offers flexibility of control over morphology, porosity, functionality and composition.

The present study takes up the mass transfer and kinetic isothermal model analysis of the Hg^{2+} adsorption results obtained using lab synthesized electrospun titania nanofibers. Mass transfer mechanism is discussed in details via Weber and Morris and Boyd models. The adsorption data is dynamically studied through Langmuir, Freundlich and Temkin isotherm models. A brief comparison with previously published works has been presented.

2 Material and methods

2.1 Nano fiber preparation

Titania nanofibers (TNF) were synthesized using a combination of sol gel and electrospinning techniques. Sol prepared with Titanium Tetraisopropoxide, ethanol and acetone in a fixed ratio was injected to a syringe and the fibers were collected at the collecting plate. After hydrolysis at room temperature, the fibers were calcined in muffle furnace. The fiber synthesis process is described in details in our previous work [12].

2.2 Adsorption experiments

Analytical grade $HgCl_2$ was used to prepare Hg^{2+} stock solution. The Hg^{2+} adsorption studies were carried out in batch mode at varying parameters. Measured quantities of TNF were dosed in Hg^{2+} aqueous solutions, and pH of the solution was varied between 4-8. The aliquots at the outlet were tested for remaining Hg^{2+} at different time intervals using ICP technique. The amount of metal ion at equilibrium, qe and % metal removal is calculated from the mass balance equation given in (1) and (2) respectively [13].

$$qe = \frac{(C_0 - C_e)}{W} \times V \quad (1)$$

$$\% R = \frac{(C_0 - C_e)}{C_0} \times 100 \quad (2)$$

where, V is the volume of the solution, W is the weight of the adsorbent, C_0 and C_e are the initial and equilibrium metal concentrations respectively.

3 Results and discussion

The fiber synthesis carried out with varying process parameters revealed morphological and chemical changes. At the most optimized conditions, perfectly smooth and well-aligned fibers with BET surface area of 740 m^2/g were observed. A surface area as large as this was sufficient enough for heavy metal adsorption application.

Fig. 1 represents the smooth surface morphology and average diameter of the synthesized TNF. Fiber morphology and chemical composition results are discussed in details in our previous work [12]. Batch experiments for Hg^{2+} adsorption were performed and effect of various parameters were studied. The pH was varied in the range 4-8, and the maximum removal was obtained at the pH value of 6.

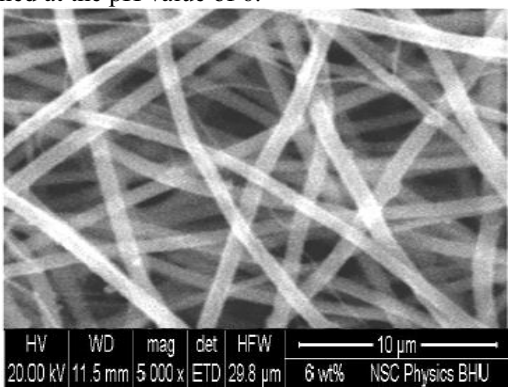

(a)

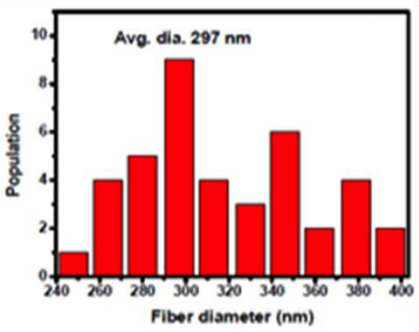

(b)

Figure 1. (a) SEM image (b) average diameter of TNF calcined at 500°C

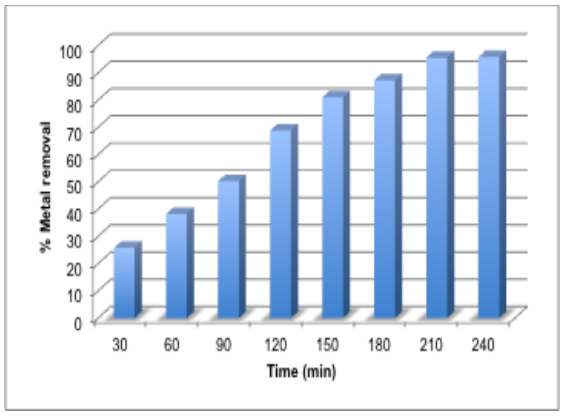

Figure 2. Hg^{2+} adsorption on TNF at different time intervals (TNF 0.05 g/L; pH 6)

3.1 Effect of contact

Fig. 2 shows the change in adsorption efficiency of the system with time, keeping the titania nanofiber dose and system pH to 0.05g/L and 6, respectively. A fast initial

adsorption rate is observed up to 150 minutes, which thereafter slows down and remains constant after 210 minutes. This phenomenon is attributed to the initial availability of greater number of vacant sites for metal ions, which apparently decreases as the time increases and finally becomes constant as the equilibrium is achieved.

3.2 Mass transfer mechanism

The rate-limiting step (slowest step of the reaction) is an important factor to be determined so as to establish the mechanism involved for transportation of mass. It may be either the boundary layer (film) or the intra-particle (pore) diffusion of solute on the solid surface from bulk of the solution in a batch process. Different steps viz. solute transfer to the sorbent surface, transfer from the sorbent surface to the active sites and retention on of metal ions on these sites via sorption, complexion and intra-particle precipitation control the sorption kinetics.

Weber and Morris suggested the probability of intra-particle diffusion, as (3). The plot of q_t versus $t^{0.5}$ represents intra-particle diffusion, where q_t represents adsorption capacity at any time t and k_i is intra-particle diffusion rate constant (mg/g $min^{1/2}$).

$$q_t = k_i\sqrt{t} \quad (3)$$

The deviation of the plot from the linearity would indicate the rate-limiting step should be boundary layer (film) diffusion controlled, that is, if the plots are not completely linear, and more-so do not pass through the origin, then intra-particle diffusion could not be the only mechanism involved. In most cases the plot features three stages; initial curved portion due to external mass transfer, followed by an intermediate linear portion due to intra-particle diffusion and a plateau to the equilibrium stage where intra- particle diffusion starts to slow down due to extremely low solute concentrations in the solution. Fig. 3(a) depicts the intra-particle plot for Hg^{2+} adsorption on TNFs. Even though the plot shows an impressive regression value (R^2 = 0.939), it can be seen that the plot is not linear over the whole time range and the graph reflects a dual nature, with initial linear portion followed by plateau. This implies that the external surface adsorption is absent. The stage of intra-particle diffusion is attained and continues till 210 min and finally, equilibrium adsorption starts after 210 min. However, the linear portion of the curve does not pass through the origin and the latter stage of adsorption does not obey Weber–Morris equation. It may be concluded that the adsorption mechanism of these ions from aqueous solution is rather complex process and the intra-particle diffusion was not the only rate-controlling step.

To investigate the mechanism of adsorption, data were fit into Boyd kinetic model [14]. It was originally proposed for intra particle diffusion in spherical particle and is basically a film diffusion model, better known as Boyd's film diffusion model. (4) represents the Boyd kinetic model where F (q_t/q_e) is the fractional attainment of equilibrium at time t, B is the Boyd constant, q_t and q_e are the amounts of metal ion adsorbed at time and at equilibrium, respectively.

$$F = 1 - \frac{6}{\pi^2}\sum_{n=1}^{\infty}\frac{1}{n^2}\,e^{-n^2Bt} \quad (4)$$

Ideally, the mechanism can be called film controlled if the plot of Bt versus time is linear and passes through origin. However, from Fig. 3(b) it can be seen that plot is not completely linear and does not pass through the origin. Also the regression value (R^2 = 0.847) obtained is not very promising. The rate control mechanism of the process does not set well with Boyd model. When a comparison is made between the intra-particle model and Boyd model based on their regression values, intra-particle model shows a better fit. This system seems to follow a complex process with none of the single mechanism taking the complete charge.

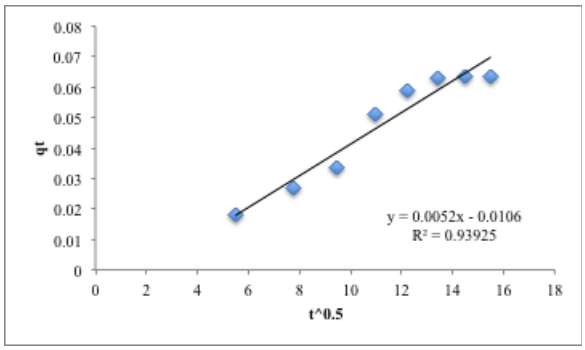

(a)

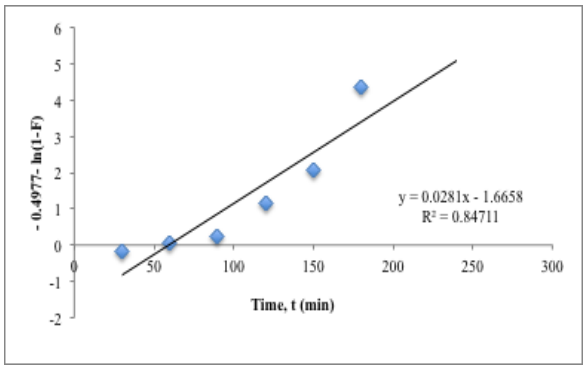

(b)

Figure 3. Mass transfer mechanism model (a) Weber and Morris (b) Boyd

3.3 Adsorption kinetics

Adsorption isotherms are empirical models representing the amount of material bound at the surface as a function of material present in bulk at constant temperature. Langmuir isotherm represents monolayer adsorption and the equation follows Henry's law. It also assumes that each site has same level of energy and the adsorbed molecules have no interaction with each other. Freundlich model assumes multilayer adsorption and Temkin

isotherm takes into account adsorbate interactions. Eq (5), (6) and (7) represents Langmuir, Freundlich and Temkin models respectively where, Q_m and Q_e represents the maximum amount of metal ion adsorbed and metal ion adsorbed at equilibrium, C_e is the metal concentration at equilibrium, k_L is Langmuir constant, k_f Freundlich constant and B is Temkin contant.

$$\frac{C_e}{Q_e} = \frac{1}{Q_m k_L} + \frac{C_e}{Q_m} \quad (5)$$

$$Log\ Q_e = Log\ k_f + \frac{1}{n}\ Log\ C_e \quad (6)$$

$$Q_e = B\ Ln\ A + B\ Ln\ C_e \quad (7)$$

The applicability of these isotherms on adsorption data was adjudged by their regression correlation coefficient, R^2, presented in Table 1. From the table it can be seen that the regression values for both Langmuir and Freundlich are impressive but best linear fit is observed by Freundlich isotherm with highest regression value of 0.991 compared to 0.964 and 0.890 by Langmuir and Temkin models respectively. The factor R_L and 1/n represents the favorability of the process through Langmuir and Freundlich, respectively. When $R_L > 1$, the reaction is unfavorable, R_L = 0-1 represents favorable conditions and R_L = 1 represents linear relationship. The value of favorability factor is close to 1 in case of Langmuir and is well within the favorable limits in case of Freundlich isotherm. The value of constant is also impressive.

Table 1. Isotherm model parameters

Langmuir	
Q_m	6.544
k_L	0.038
R_L	0.989
R^2	0.964
Freundlich	
1/n	0.453
k_f	0.174
R^2	0.991
Temkin	
A	0.054
B	0.241
R^2	0.890

3.4 Comparison with similar works

Numerous earlier works have used nano-sized adsorbents for removing Hg^{2+} from aqueous solutions in batch experiments. Table 2 represents some of the recent works on mercury adsorption in batch mode using nano adsorbents. Manganese chloride nanoparticles [15], functionalized iron nanoparticles [16-18] with particle diameters 100, 40-50 and 10 nm respectively could remove more than 95% Hg(II) at various concentrations. Titania nano particles [19, 20] with diameter ranging from 3-10 nm and large surface area had adsorption capacity of more than 120 mg/g Hg(II) at concentrations ranging from 100-800 mg/L with or without UV illumination. More than 90% of 40-100 ppm Hg(II) in aqueous media was removed by thiol functionalized magnetite nanoparticles [21]. Iron oxide nano composite [22] and nano polymer [23] showed a good affinity over a range of metal ion concentration, with adsorption efficiency around 167.8 and 256.4, respectively. Fe_2O_3-Al_2O_3 nano fibers [24] had a small surface area of 9.6 m^2/g but exhibited Hg(II) adsorption of 89%. Most of the mechanisms were second order reaction and followed Langmuir isotherm. However few works fitted well to Freundlich isotherm as well. The works mentioned above have targeted a higher Hg(II) concentration while the need of the hour is to target the concentrations close to the ones found in real industrial effluents. The lab synthesized TNF used in the present work had very high affinity for Hg^{2+} metal ions. The metal uptake in the present work went to 95.5% at Hg^{2+} concentration of 0.01ppm within 210 minutes. The main reason behind this seems to be the high surface area. Adsorption, being a surface phenomenon largely depends on surface area and with such high surface areas comes higher removal efficiencies.

Table 2. Comparison of recent works on nano adsorbents

Nano Adsorbent	Propert-ies	Working condition	Findings	Ref.
Mn(III)Cl NP on SiO_2/Al_2O_3 mixed oxide support	D = 5-30 SA = 243	C= 0.5-400, A = 0-41.5, pH = 1-12, t = 0-12, T =25-80	Q = 289.5, I- Langmuir Freundlich O- Second	15
Fe_3O_4-Hydroxyapatite NP	D = 100	C = $2.5e^{-8}$, A = 0.1-4, pH = 3-9, t = 0-1, T = 10-40, S = 200	R = 98, I- Langmuir O- Second	16
Fe_3O_4 NPs modified with 2-mercaptobenzothiazole	D = 40-50	C = 20-100 ng/L, A = 0.06-2.4, pH = 1-11, t = 0-0.5	R = 98.6 I- Langmuir	17
Polyrhodanine-coated γ-Fe_2O_3 NPs	D = 10 SA = 94.65	C = 1-80, A = 0.5, pH = 2-8, t = 0-12, T = 25	R = 94.5 I- Freundlich O- Second	18
TiO_2 NP	D = 10.19 SA = 98.74	C = 100-800, A = 1-5, pH = 2-9, t = 0.5-9, T = 30-60	Q = 166.66 I- Freundlich, O- Second	19

TiO_2 NPs (+ UV)	D = 9.1 SA > 200	C = 100, A = 10, pH = 6, t = 1.5, T = 25-45	Q = 101 E_a = 25 I-Langmuir O-First	20
TiO_2/montmorillonite (+ UV)	D = 3.1 SA = 239		Q = 123.8 Ea = 22.6 I-Langmuir O-First	
Thiol-functionalized silica-coated magnetite NPs	D = 50	C = 40-100 µg/L, A = 4-8 mg/L, pH = 2-9, t = 0.25, T = 10-35	R = 93.76 I-Freundlich	21
Amino functionalized Fe_3O_4 graphene NC	D = 38.57 SA = 62.43	C = 3, A = 0.16, pH = 1-9, t = 0-5, T = 20-40	Q = 167.8 I-Langmuir O-Second	22
Mercapto functionalized nano-magnetic Fe_3O_4 polymers	D = 40	C = 20-100, A = 0-1, pH = 2-6, t = 0-3, T = 25-45	Q = 256.4, I-Freundlich O-Second	23
Fe_2O_3-Al_2O_3 NF	D = 200-500 SA = 9.6	C = 5-50, A = 2.5, pH = 2-8, t = 0-3, T = RT	R = 89, I-Langmuir O-Second	24

 # NC-Nano composite; NF-Nano fiber; NP-Nano particle; D-Diameter (nm); SA-Surface area (m^2/g) ; C-Hg(II) concentration ; A-Adsorbent dose ; t-time (hours) ; T-Temp (℃) ; Q-Adsorption capacity (mg/g) ;R Removal % ; I-Isotherm ; O-Order

4 Conclusion

This study has shown the applicability of titania nanofibers for Hg^{2+} uptake from aqueous solutions. The adsorption of metal ion was found to be dependent on pH and contact time apart form other factors. The work highlights an enhanced rate of adsorption, which is attributed to the large surface area. The TNFs possessed a surface area of 740 m^2/g characterized by BET. A detailed discussion on mass transfer mechanism, taking into picture both intra particle and film diffusion control is taken up. The nature of the plot indicated that the mass transfer process is rather complex. Langmuir, Freundlich and Temkin isotherms were tested and the constant values, favorability factor and regression values all indicated the suitability of freundlich isotherm model. TNF showed a great affinity for Hg^{2+} and can be a potential candidate for adsorption of other metals as well.

References

1. M. Firouzzare, Q. Wang, Talanta. **101**, 261-266 (2012)
2. K. Kadirvelu, M. Kavipriya, C. Karthika, N. Vennilamani, S. Pattabhi, Carbon. **42**, 745-752 (2004)
3. X. Liu, Q. Hu, Z. Fang, X. Zhang, B. Zhang, Langmuir. **25**, 3-8 (2009)
4. R. O. Long, R. T. Yang, J. Am. Chem. Soc. **123**, 2058-2059 (2001)
5. G. N. Chaudhari, D .R. Bambole, A. B. Bodade, J. Mater. Sci. **41**, 4860-4864 (2006)
6. C. L. Chen, H. S. Weng, Appl. Catal. B-Environ. **55**, 115-122 (2005)
7. S. J. Park, S. Bhargava, E. T. Bender, J. Mater. Res. **23**, 1193-1196 (2008)
8. T. Matsui, M. Harada, Y. Ichihashi, Appl. Catal. A-Gen. **286**, 249-257 (2005)
9. V. Tomer, R. Teye-Mensah, J. C. Tokash, Sol. Energy Mater. Sol. Cells. **85**, 477-488 (2005)
10. S. K. Pradhan, P. J. Reucroft, F. Yang, J. Cryst. Growth. **256**, 83-88 (2003)
11. J. Yang, S. Mei, J. M. F. Ferreira, J. Am. Chem. Soc. **84**, 1696-1702, 2001.
12. A. Dixit, K. Atal, P. K. Mishra, M. S. Alam, Asian J. Chem. **28**, 2, 415-422 (2016)
13. B. H. Hameed, A. M. Din, A. L. Ahmad, J. Hazard. mater. **137**, 3, 695-699 (2006)
14. G. E. Boyd, A. W. Adamson, L. S. Myers-Jr., J. Am. Chem. Soc., **69**, 2836-2848 (1947)
15. M. Arshadi, Chem Eng J. **259**, 170-182 (2015)
16. Kh. Hardani, F. Buazar, K. Ghanemi, M. Kashisaz, M. H. Baghlani-Nezhad, A. Khaledi-Naseb, M. Badri, Amer. Assoc. Sci. Tech. J. Nanosci. **1**, 1, 11-18 (2015)
17. H. Parham, B. Zargar, R. Shiralipour, J. Hazard. mater. **205-206**, 94-100 (2012)
18. J. Song, H. Kong, J. Jang, J. Colloid Interface Sci. **359**, 505-511 (2011)
19. Z. Ghasemi, A. Seif, T. S. Ahmadi, B. Zargar, F. Rashidi, G. M. Rouzbahani, Adv Powder Technol. **23**, 148-156 (2012)
20. B. Dou, V. Dupont, W. Pan, B. Chen, Chem Eng J. **166**, 631–638 (2011)
21. O. Hakami, Y. Zhang, C. J. Banks, Water Res., **46**, 12, 3913-3922 (2012)
22. X. Guo, B. Dua, Q. Wei, J. Yang, L. Hu, L. Yan, W. Xua, J. Hazard. mater. **278**, 211-220 (2014)
23. S. Pan, Y. Zhang, H. Shen, M. Hu, Chem Eng J. **210**, 564-574 (2012)
24. A. Mahapatra, B. G. Mishra, G. Hota, J Hazard Mater. **258- 259**, 116-123 (2013)